Zahirovic Selma, Scharler Robert, Obernberger Ingwald, 2006: Advanced CFD modelling of pulverised biomass combustion. In: Proceedings of the International Conference Science in Thermal and Chemical Biomass Conversion, Sept 2004, Victoria, Canada, ISBN 1-872691-97-8, pp.267-283, CPL Press (Ed.)

Advanced CFD modelling of pulverised biomass combustion

S. Zahirovic, R. Scharler, I. Obernberger
Institute for Ressource Efficient and Sustainable Systems, Graz University of Technology, Graz, Austria
Inffeldgasse 25, A - 8010 Graz, Austria; Tel.: +43 (0)316 481300 32, Fax: +43 (0)316 481300 4; E-mail: zahirovic@rns.tugraz.at

ABSTRACT: In this paper, the development and application of a CFD model for pulverised biomass combustion is presented. As a first step, the Discrete Phase Model (DPM) of the commercial CFD software FLUENT, originally developed for the combustion of pulverised coal, was investigated regarding its capability to predict pulverised biomass combustion. Based on these investigations, a more detailed sub-model for the devolatilisation part of the combustion process, was included. Furthermore, the original DPM energy equation for a single particle was modified in order to account for the temperature-dependent specific heat capacity of a particle. This modification allows for a more accurate prediction of the temperature of a single particle (until the inert state of fly ash) along its trajectory. The validation of the modified DPM for thermally thin particles was performed with a 2 D numerical simulation of a pulverised wood flame in a vertical tube furnace.
As a first engineering application, a 3D simulation of a wood dust-fired biomass underfeed stoker furnace was successfully performed. During operation it was observed, that a part of the fuel particles, which were apparently too small for fixed bed combustion, were entrained and burned out “on-the-fly”. This effect seemed to be the reason for high temperatures and ash slagging at the upper wall of the primary combustion chamber. In order to investigate this phenomenon, the extended DPM was applied in combination with an earlier developed CFD model for biomass grate furnaces. With the simulations performed, the entrained fuel particles could be identified to be the reason for the slagging problems.
The developed model showed to be a valuable design tool for pulverised biomass combustion furnaces, but further extensions of the model are necessary and ongoing in order to appropriately describe the particle combustion process.

INTRODUCTION

CFD analysis has been successfully applied for the design and optimisation of several biomass grate furnaces [10, 12]. Being interested in applying the same tool in a numerical study of pulverised biomass furnaces, the Discrete Phase Model (DPM) of the commercial CFD software FLUENT 6 was investigated regarding its capability to predict pulverised biomass combustion. The DPM, originally developed for the combustion of pulverised coal, is based on the assumption of thermally thin particles.

In order to describe the processes of drying, devolatilisation and char combustion of a single fuel particle, the DPM utilises a set of sub-models, considered to proceed one after another.

On the basis of the Biot number, which relates the internal heat transfer resistance to the external heat transfer resistance, particles can be generally divided into two categories: thermally thick and thermally thin ones. In the latter case the conduction effects can be neglected and the temperature throughout the particle can be considered to be uniform. The modelling work, done within the present study, is based on this assumption. It is postulated that for thermally thin particles the stages of the thermal conversion occur in series. But even for combustion of thin coal particles under some conditions the devolatilization and the char combustion can proceed in parallel [5]. In contrast to coal, wood is a fibrous solid, thus it cannot be easily reduced in size [9]. The size range of pulverised wood particles overcomes greatly those of pulverised coal and, hence, lay partly in the thermally thick range.

Despite the general similarities between pulverised combustion of coal and that of biomass, which make much of the information available for coal transferable to biomass combustion [16], major differences have to be considered for modelling of combustion of biomass particles. Compared to coal, biomass has a much higher amount of volatile matter (approximately 80% and more), resulting in a dominating role of devolatilisation in the overall conversion process of the biomass particles. Therefore, a biomass-specific sub-model for devolatilisation has been incorporated in the original DPM. For drying and char combustion the original DPM sub-models have been applied.

Moreover, concerning problems related to deposit formation and ash melting behaviour, the correct prediction of the particle temperature is of key importance. In the original DPM the temperature of a single combusting particle is calculated, assuming the constant value of the specific heat capacity of the solid fuel. Implying the temperature-dependent empirical correlations for the specific heat capacity of the solid biomass particle from [4], the energy equation for a single particle was modified.

The validation of the modified DPM was performed based on a 2D simulation of a pulverised wood flame in a vertical tube furnace. Furthermore, the applicability of the modified DPM for technical problems was investigated in a 3D simulation of a wood dust-fired biomass underfeed stocker furnace. During operation of this furnace it was observed, that a part of the fuel particles, which were apparently too small for fixed bed combustion, were entrained and burned out “on-the-fly”, resulting in high temperatures and ash slagging at the upper wall of the primary combustion chamber. In order to investigate this phenomenon, the extended DPM was applied in combination with an earlier developed CFD model for biomass grate furnaces. With the simulations performed, the entrained fuel particles could be identified to be the reason for the slagging problems.

Although all simulation results are satisfying, they indicate the necessity of modelling thermally thick biomass particles. The work on this issue is part of ongoing research and is not included in the present study.

MODELLING

Modelling of pulverised wood combustion within FLUENT 6 follows an Euler-Lagrange approach. The gas phase is treated as continuum and described by the time-

averaged equations for mass, momentum, energy and species fractions, formulated in an Eulerian frame of reference. The discrete phase equations are formulated in a Lagrangian frame of reference. The coupling between the phases, i.e. the exchange of mass, heat and momentum is introduced through source terms in all equations for gas phase.

MODELLING OF PULVERISED BIOMASS COMBUSTION

The equation set for pulverised biomass combustion consists of the equation of motion for a particle, the energy transfer equation and the mass transfer equation. The original formulation of the equation of motion is applied during the whole combustion process (see [3] for details). The sub-models for initial heat-up, drying, devolatilisation, char combustion and final heating/cooling of the ash include heat and mass transfer equations. Within the present work, the simulations were performed with the following combustion sub-models:

(1) The stage of the initial heat–up follows the inert law of the original DPM. During this stage the particle mass stays constant and the particle temperature is calculated from the modified FLUENT DPM energy equation.
(2) The drying of a single fuel particle is modelled by two subsequent steps, vaporisation and boiling (according to the vaporisation law and boiling law of the original DPM). The mass loss during drying is calculated via original DPM equations. The temperature of the particle is determined from the modified FLUENT DPM energy equation.
(3) During the process of devolatilisation the mass loss follows a biomass-specific sub-model, described below. The sub-model remains in effect as long as the mass of the particle exceeds the mass of the char. The solution of the modified FLUENT DPM energy equation gives the temperature of the particle.
(4) The char combustion follows the surface combustion law of the original DPM. The biomass char is assumed to consist only of carbon and oxidises according to

$$char + S_b \cdot O_2 \rightarrow CO_2 \tag{1}$$

where S_b [-] is the burnout stoichiometric ratio. The surface reaction proceeds at the rate given by the diffusion-limited surface reaction model (a part of the original DPM) until the combustible fraction is consumed. The particle temperature is calculated from the modified FLUENT DPM energy equation.
(5) The stage of final heating/cooling of the ash follows the inert law of the original DPM. The solution of the modified FLUENT DPM energy equation delivers the temperature of the remaining ash.

Modified heat transfer equation

Assuming thermally thin particles FLUENT solves the following heat transfer equation

$$m_p c_p \frac{dT_p}{dt} = \underbrace{hA_p(T_\infty - T_p)}_{convection} + \underbrace{\varepsilon_p A_p \sigma(\theta_R^4 - T_p^4)}_{radiation} + \underbrace{Q^{(i)}}_{add.\,sink/source}, \tag{2}$$

which relates the particle temperature, $T_p(t)$ [K], to the convective heat transfer, absorption/emission of radiation at the particle surface and an additional heat sink or source, $Q^{(i)}$ [W]. The formulation of $Q^{(i)}$ depends on the mass loss at the stage of the thermal conversion, a single particle is going through. In equation (2), m_p [kg] is the mass of the particle, c_p [J/kgK] is the specific heat capacity of the particle, A_p [m^2] is the surface area of the particle, T_∞ [K] is the local temperature of the gas phase, h [W/m^2K] is the convective heat transfer coefficient, calculated from the correlation of Ranz and Marshall [3], ε_p = 0.9 [-] is the particle emissivity (value taken from [2, 3]), $\sigma = 5.67 \cdot 10^{-8}$ [W/m^2K^4] is the Stefan-Boltzmann constant and θ_R [K] is the radiation temperature of the surroundings.

The original DPM is based on constant specific heat capacities of both the liquid water $c_{p,w}$ [J/kgK] and the specific heat capacity of the solid dry substance $c_{p,dw}$ [J/kgK]. During initial heat-up and drying, the specific heat capacity of the wet particle is calculated as a mass fraction average of the specific heat capacities $c_{p,w}$ and $c_{p,dw}$. For the stages of devolatilisation, char combustion and final heating/cooling of the remaining ash the original DPM applies a constant value, $c_{p,dw}$.

In the present work, the specific heat capacity of the particle is varied in dependence of the particle temperature and the conversion stage. A mass fraction average of the specific heat capacities $c_{p,w}$ and $c_{p,dw}$ gives the value of the specific heat of the particle at the stage of drying. During devolatilisation, it is assumed that the specific heat of the particle varies linearly between the specific heat capacity of the dry virgin wood $c_{p,dw}$ and that of the char $c_{p,c}$. During char combustion, the specific heat of the particle follows the linear variation between the specific heat of the char $c_{p,c}$ and that of the ash $c_{p,a}$. In both cases, an interpolation factor η [–] is introduced, which relates the unconverted part of the particle mass to the total particle mass that can be converted at a certain stage of conversion. Table 1 summarises the input parameters for the energy equation.

Devolatilisation sub-model

In the presented work, the devolatilisation process was modelled following the independent parallel reactions approach, employed in several studies for modelling devolatilisation of biomass under different conditions [4, 6, 15]. The main difference of the independent parallel reactions model compared to devolatilisation sub-models provided by FLUENT, is the assumption that the three main components of wood, cellulose, hemicelluloses and lignin decompose separately to volatiles and char:

$$\left.\begin{aligned} c_1 \cdot wood &\xrightarrow{k_1} \\ c_2 \cdot wood &\xrightarrow{k_2} \\ c_3 \cdot wood &\xrightarrow{k_3} \end{aligned}\right\} \underbrace{f_{v,0} \cdot CH_xO_y}_{volatiles} + \underbrace{f_{c,0} \cdot C}_{char} . \qquad (3)$$

The conversion rate k_i [1/s] of each component is approximated by an Arrhenius equation. The coefficients c_i [-] represent the amount of volatiles produced by the ith component. In the present work, the value of the fraction of the total amount of volatiles $f_{v,0}$ [wt% d.b.] is assumed to equal the fraction of volatiles given by the proximate analysis of the fuel. The char is assumed to consist of pure carbon and the

value of the char fraction $f_{c,0}$ [wt% d.b.] is given by the amount of fixed carbon according to the proximate analysis of the fuel. All model parameters are given in Table 2.

The main disadvantage of the independent parallel reactions model is that the coefficients c_i and the kinetic parameters (pre-exponential factor A_i and activation energy E_i) are determined from thermogravimetric analysis (TGA). The parameters c_i, A_i and E_i are strictly valid only for the conditions, under which the TGA experiment was performed, and for the distribution of the devolatilisation products (volatiles and char), resulting from the respective TGA test run.

Since in FLUENT only one species, CH_xO_y can be released from the particle surface during devolatilisation, an artificial reaction was added to the reaction mechanism for the gas phase

$$CH_xO_y \rightarrow \sum_{i=1}^{n} \nu_i \cdot P_i \,, \tag{4}$$

introduced only for the purpose of modelling the composition of volatile gases P_i, leaving the surface of the particles (CH_4, CO, CO_2, H_2 and H_2O in this case). The distribution of gas species (coefficients ν_i) in volatiles was determined from chemical equilibrium calculations. These calculations were performed in a temperature range T_{devol} = 700 - 900 [K], in which the most of the volatiles are released under rapid devolatilisation conditions as proven experimentally in [8].

The effect of the shrinkage of a single fuel particle during the devolatilisation process is modelled by means of the constant C_{sw} [-] (termed in FLUENT as swelling coefficient). In the present work the value of C_{sw} is calculated from

$$C_{sw} = \left[\frac{(1 - f_{v,0})\rho_{dw}}{\rho_{char}} \right]^{1/3} , \tag{5}$$

where $f_{v,0}$ [wt% d.b.] is the fraction of the total amount of volatiles initially present in the particle, ρ_{dw} [kg/m^3] is the density of the dry virgin wood and ρ_{char} [kg/m^3] is the density of the char after the devolatilisation process is completed (see Table 2). The change of the particle diameter is given by

$$\frac{d_p}{d_{p,0}} = 1 + (C_{sw} - 1)\frac{(1 - f_{w,0})m_{p,0} - m_p}{f_{v,0}(1 - f_{w,0})m_{p,0}} , \tag{6}$$

according to [3]. In equation (6) d_p [m] is the current particle diameter and $d_{p,0}$ [m] is the particle diameter at the start of the devolatilisation process.

Table 1 Values and correlations of physical parameters used as input for the energy equation (1) in different stages of combustion.

parameter	correlation/value	unit	ref.
specific heat capacity of liquid water	$c_{p,w} = 4{,}812$	J/kgK	[3]
specific heat capacity of dry virgin wood [1)]	$c_{p,dw} = 1{,}500 + T_p$	J/kgK	[4]
specific heat capacity of char [2)]	$c_{p,c} = 420 + 2.09T_p + 6.85 \cdot 10^{-4} T_p^2$	J/kgK	[4]
specific heat capacity of ash [3)]	$c_{p,a} = 1{,}100$	J/kgK	
initial heat-up			
heat source	$Q^{(heat-up)} = 0$	W	[3]
specific heat capacity of moist wood	$c_p^{(heat-up)} = f_{w,0} c_{p,w} + (1 - f_{w,0}) c_{p,dw}$	J/kgK	[3]
drying			
heat source	$Q^{(drying)} = \frac{dm_p^{(drying)}}{dt} h_w$	W	[3]
latent heat of water	$h_w = 2.263 \cdot 10^6$	J/kg	[3]
specific heat capacity of moist wood	$c_p^{(drying)} = f_w c_{p,w} + (1 - f_w) c_{p,dw}$	J/kgK	[3]
devolatilisation			
heat source	$Q^{(dev)} = \frac{dm_p^{(dev)}}{dt} h_{vol}$	W	[3]
latent heat of volatiles [4)]	$h_{vol} = 0$	J/kg	
specific heat capacity of the solid substance	$c_p^{(dev)} = \eta^{(dev)} c_{p,dw} + (1 - \eta^{(dev)}) c_{p,c}$	J/kgK	[4]
interpolation factor	$\eta^{(dev)} = \frac{m_p}{(1 - f_{w,0}) f_{v,0} m_{p,0}}$	-	
char combustion			
heat source	$Q^{(comb)} = -f_h \frac{dm_p^{(comb)}}{dt} H_{reac}$	W	[3]
heat of reaction for burnout	$H_{reac} = 3.2789 \cdot 10^7$	J/kg	[3]
heat fraction absorbed by solid	$f_h = 0.2$	-	[15]
specific heat capacity of the solid substance	$c_p^{(comb)} = \eta^{(comb)} c_{p,c} + (1 - \eta^{(comb)}) c_{p,a}$	J/kgK	
interpolation factor	$\eta^{(comb)} = \frac{m_p}{(1 - f_{w,0})(1 - f_{v,0}) m_{p,0}}$	-	
final heating/cooling of the ash			
heat source	$Q^{(final)} = 0$	W	[3]
specific heat capacity of the remaining ash	$c_p^{(final)} = c_{p,a}$	J/kgK	

Explanations: 1)…correlation valid in the range from 350 to 500 [K]; 2)…correlation valid in the range from 273 to 1,273 K; 3)…assumed in present work; 4)…the endothermicity of the devolatilisation process was neglected; m_p…current mass of particle, [kg]; $m_{p,0}$…initial mass of particle, [kg]; f_w…current water content [wt% w.b.]; $f_{w,0}$…initial water content [wt% w.b.]; $f_{v,0}$…initial volatile content [wt% d.b.].

Table 2 Parameters used for the devolatilisation sub-model [4].

property	correlation/value	unit
hemicellulose	$k_1 = A_1 \exp(-E_1 / RT_p)$	1/s
amount of volatiles produced	$c_1 = 0.45$	-
pre-exponential factor	$\log A_1 = 6.98$	$\log s^{-1}$
activation energy	$E_1 = 106.9$	kJ/mol
cellulose	$k_2 = A_2 \exp(-E_2 / RT_p)$	1/s
amount of volatiles produced	$c_2 = 0.34$	-
pre-exponential factor	$\log A_2 = 20.86$	$\log s^{-1}$
activation energy	$E_2 = 276.5$	kJ/mol
lignin	$k_3 = A_3 \exp(-E_3 / RT_p)$	1/s
amount of volatiles produced	$c_3 = 0.21$	-
pre-exponential factor	$\log A_3 = 0.56$	$\log s^{-1}$
activation energy	$E_3 = 44.2$	kJ/mol
density of dry wood	$\rho_{dw} = 470$	kg/m3
density of char	$\rho_c = 290$	kg/m3

Explanations: the amount of volatiles c_i produced is expressed on the basis of the total amount of volatiles; all values given relate to spruce.

MODELLING OF THE GAS PHASE

The modelling of the turbulent reactive flow is based on the Realizable k-ε Model (turbulence), the Discrete Ordinates Model (radiation) and the Eddy Dissipation Model (turbulent gas phase combustion) in combination with a global methane 3-step reaction mechanism of Brink [1] considering the species CH_4, CO, CO_2, H_2, H_2O and O_2.

The Eddy Dissipation Model (EDM) in combination with reaction kinetics serves to calculate the rate of fuel consumption R_{br} [kg/m^{3}s] as the lowest (limiting) step of mixing rates proportional to the decay of fuel, oxygen and product swirls as well as a kinetic rate $R_{br,kin}$ [kg/m^{3}s] without consideration of the influence of turbulent fluctuations

$$\overline{R_{br}} = MIN\left(\underbrace{A_{mag}\,\overline{\rho}\,\frac{\tilde{\varepsilon}}{\tilde{k}}\,\tilde{Y}_{br}}_{decay\ of\ fuel\ eddies},\ \underbrace{A_{mag}\,\overline{\rho}\,\frac{\tilde{\varepsilon}}{\tilde{k}}\,\frac{\tilde{Y}_{ox}}{r_f}}_{decay\ of\ oxygen\ eddies},\ \underbrace{A_{mag}\,B_{mag}\,\overline{\rho}\,\frac{\tilde{\varepsilon}}{\tilde{k}}\,\frac{\tilde{Y}_{prod}}{(1+r_f)}}_{decay\ of\ product\ eddies},\ \overline{\underbrace{R_{br,kin}}_{kinetic\ term}} \right). \quad (7)$$

In equation (7), A_{mag} and B_{mag} are empirical constants of the EDM, k [m^2/s^2] is the Favre-averaged turbulent kinetic energy, ε [m$^{2/}$s^3] is the Favre-averaged dissipation rate of turbulent kinetic energy, Y [-] is the Favre-averaged mass fractions of fuel (f), oxidiser (ox) or product (prod), respectively, and r_f is the mass-weighted stoichiometric coefficient of the fuel.

The EDM is reasonably accurate for most industrial applications, numerically robust and applicable to premixed, non-premixed and partially premixed combustion but cannot account for strong coupling between turbulence and multi-step chemistry. Another disadvantage is the fact that the originally proposed value of the empirical model parameter, A_{mag} = 4.0 [7], which determines the mixing rate (i.e. the reaction rate under the assumption that the combustion process is mainly mixing limited) is not universally valid. In the present study the influence of the different values of A_{mag} on the prediction of pulverised wood flames was investigated. For the simulation of the biomass underfeed stoker furnace, a value of A_{mag} = 0.6, found to be suitable for biomass grate furnaces [11, 13], was applied.

EMPIRICAL FUEL BED COMBUSTION MODELLING

For a 3D simulation of a wood dust-fired biomass underfeed stoker furnace the extended DPM was applied in combination with an earlier developed empirical model for fixed bed combustion of solid biomass fuels (see [11] for details). The empirically derived fixed bed combustion model runs in a pre-processor mode and provides the boundary conditions (mass and energy fluxes of the flue gas released from the fuel bed) for the subsequent CFD simulation of the gas phase in the furnace.

DISSCUSSION OF RESULTS

In the following the results from the validation of the extended DPM based on a 2D simulation of a pulverised wood flame in a vertical tube furnace as well as the results from a 3D simulation of a wood dust-fired underfeed stoker furnace are presented.

VALIDATION CASE – PULVERISED WOOD FLAME

The experimentally investigated vertical tube furnace [15] with an inner diameter of 0.25 [m] and a height of 4 [m] was equipped with an axial burner, installed on the top of the furnace. An axial burner was chosen for the experiments because it establishes a simple flow pattern behind it. Table 3 summarises the characteristics of the pulverised wood used in the experiment. It was made from softwood pellets ground in a mill, with a resulting particle size distribution in the range of 28.5 to 1,200 [μm] and a mean particle size d_{50} = 400 [μm], according to the data reported in [19].

Table 3 Wood powder characteristics.

moisture content	proximate analysis, wt% d.b.			ultimate analysis, wt% d.b.						net calorific value
wt% w.b.	volatiles	fixed carbon	ash	C	H	O	N	S	Cl	MJ/kg w.b.
7.8	84.7	15	0.3	50.7	6.2	42.8	<0.1	<0.01	<0.01	17.52

All calculations were performed for the operation conditions (see Table 4) of the test runs. The primary and secondary air were not pre-heated. A wall temperature profile, based on wall temperatures, which were measured at eight positions using thermocouples, was used as boundary condition for the numerical simulations.

The validation of the modified DPM was carried out by means of measured gas temperatures and the measured gas species concentrations for O_2, CO_2 and CO (as well as H_2 and ultra light hydrocarbons UHC, which are not discussed here) along the furnace axis. A detailed description of the experimental equipment and the measurement procedure can be found in [15].

Table 4 Operation conditions.

parameter	value	unit
wood powder feed rate	6	kg/h
primary air flow	12	Nm^3/h
secondary air flow	18	Nm^3/h

Discussion of results

Figs. 1-4 show the comparison of numerical and experimental results for the flame temperature as well as mole fractions of O_2, CO_2 and CO along the furnace axis.

The influence of three model parameters on the simulation results was studied. The composition of the volatiles released was determined at two different temperatures T_{devol} = 700 [K] and T_{devol} = 800 [K]. Moreover, simulations with different values of the empirical Magnussen constant A_{mag}, of the EDM, which determines the mixing rate (i.e. the reaction rate under the assumption that the combustion process is mainly mixing limited), were performed (A_{mag} = 1 and A_{mag} = 2). Additionally, the effect of the specific heat capacity c_p of the fuel particles on the gas phase as well as on the temperature of a single particle was investigated.

Generally, a good agreement between the numerically predicted and measured flame temperature could be achieved (see Fig. 1). The calculated O_2 and CO_2 concentrations follow qualitatively the measured ones (see Fig.2 and Fig. 3). In [15] the authors reported, that during the experiments they performed, the fuel supply was instable due to difficulties with the fuel feeding system. Whereas the gas temperatures were monitored using 5 fixed suction pyrometers, thus monitoring one operating condition, one moveable quench liquid probe was used for the determination of the species concentrations. Taking into account the instabilities during experiments, the measured species concentrations may correspond to different operating conditions. For this reason larger uncertainties have to be assumed for the measurement data when being compared to calculation results.

The results of a simulation performed with the one-step kinetic rate model, provided within FLUENT (parameters used for spruce wood: log$A$ = 6.18 [log s^{-1}] and E = 102.6 [kJ/mol], both from [4]) show, that the one-step kinetic rate model obviously cannot predict the release of volatiles correctly (see Figs. 1-4). It results in a too moderate increase of the gas temperature along the furnace axis without clear flame lift-off. An overall improvement in the numerical prediction was obtained by applying the independent parallel reaction model for the devolatilisation process, although a delayed temperature rise along the furnace axis is still present, compared to the measurement results. Besides the influence of the kinetic parameters used, this effect may result from the modelling assumption of thermally thin particles and a serial sequence of the devolatilisation and char combustion processes. Taking into account,

that the overlapping of the mentioned processes, which may take place, cannot be predicted with the present model, the results indicate the necessity of the consideration of thermally thick particles by resolving temperature gradients within them and thus, accounting for a possible overlap.

Among all of parameters varied, the value of A_{mag} has the strongest influence on the gas flow field calculated. The calculations with A_{mag} = 1 show a better agreement with the measured flame temperatures, CO_2 and O_2 concentrations. These findings are in agreement with [11], where the values of A_{mag} from 0.8 to 1 have been proposed as best suitable for the simulation of the gas flames. Compared to the simulation results achieved for A_{mag} = 2, the lower value A_{mag} = 1 results in lower reaction rates (eddy break-up rates), thus leading to lower peak temperatures (Fig.1) and higher CO concentrations (Fig. 4). These facts evidence, that the modelling of the gas phase combustion has a very strong influence on the overall simulation results. Therefore, more sophisticated gas phase combustion models are currently being developed.

The different composition of volatiles released from the particle surface, determined at two temperatures T_{devol}, does not have a great impact on the overall simulation results (see Figs. 1-4). Hence, the value of the presumed temperature T_{devol} influences the composition of the flue gas formed only slightly. A high discrepancy between measured and predicted concentrations of the intermediate species CO is common to all simulations (see Fig. 4). It arises due to the fact, that in the model applied the distribution of the volatiles released from the particle surface is kept constant during the process of devolatilisation.

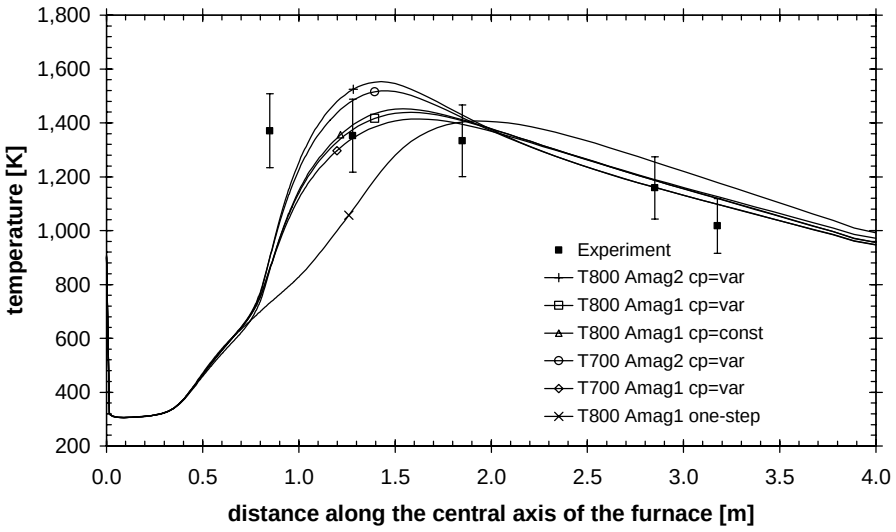

Fig. 1 Flame temperature along the furnace axis.

Explanations: Experiment….measured values of flame temperature with an uncertainty margin of 10%, [15]; T…devolatilisation temperature T_{devol}, values used: T_{devol}=700 and T_{devol}=800 [K]; Amag…Magnussen constant A_{mag}, values used: A_{mag}=1 and A_{mag}=2; cp=var…simulations performed with variable specific heat capacity of the fuel particles; cp=const…simulation performed with constant specific heat capacity of the fuel particles c_{sd} = 1,700 [J/kgK]; one-step…simulation performed with the one-step kinetic model.

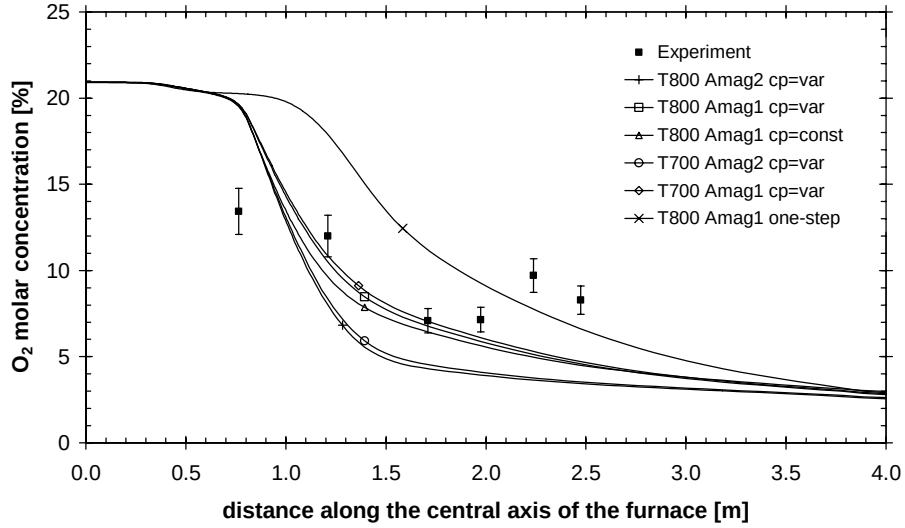

Fig. 2 O_2 concentration along the furnace axis.
Explanations: Experiment...measured values of O_2 concentrations with an uncertainty margin of 15%, [15]; for abbreviations see Fig.1.

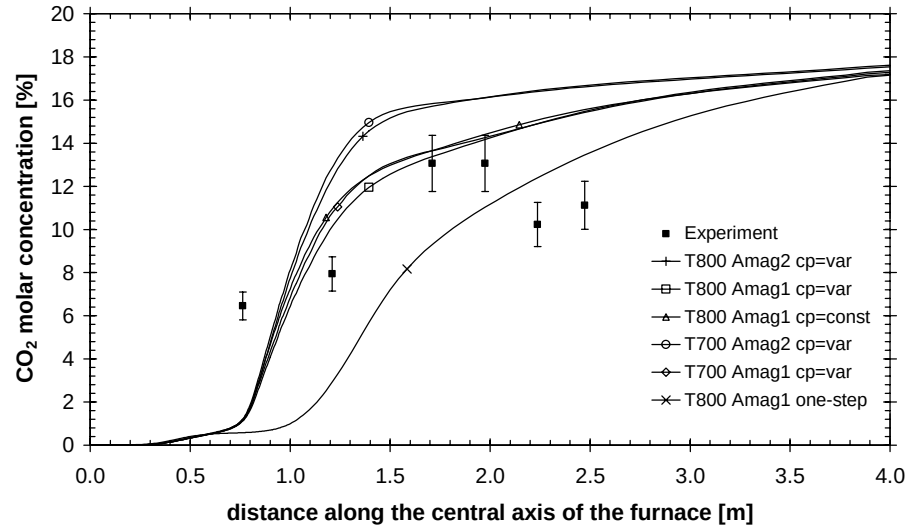

Fig. 3 CO_2 concentration along the furnace axis.
Explanations: Experiment…measured values of CO_2 concentrations with an uncertainty margin of 15%, [15]; for abbreviations see Fig.1.

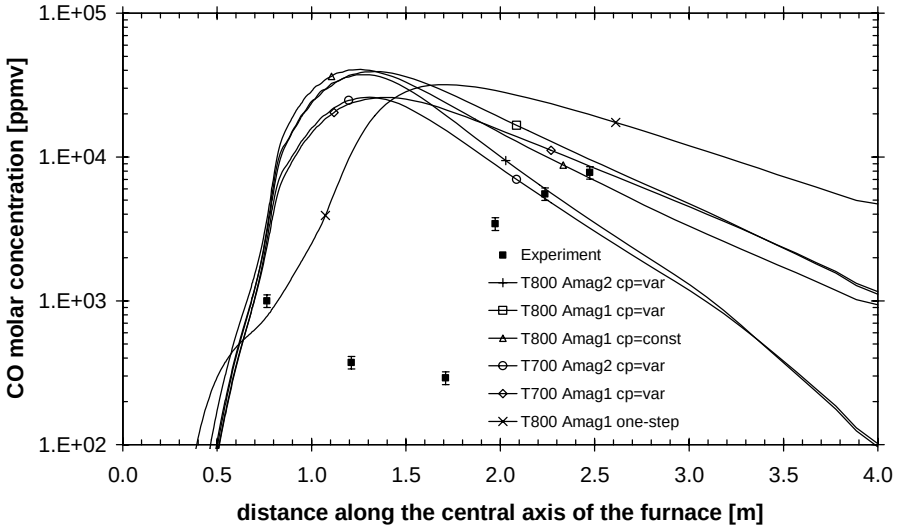

Fig. 4 CO concentration along the furnace axis.
Explanations: Experiment…measured values of CO concentrations with an uncertainty margin of 30%, [19]; for abbreviations see Fig.1.

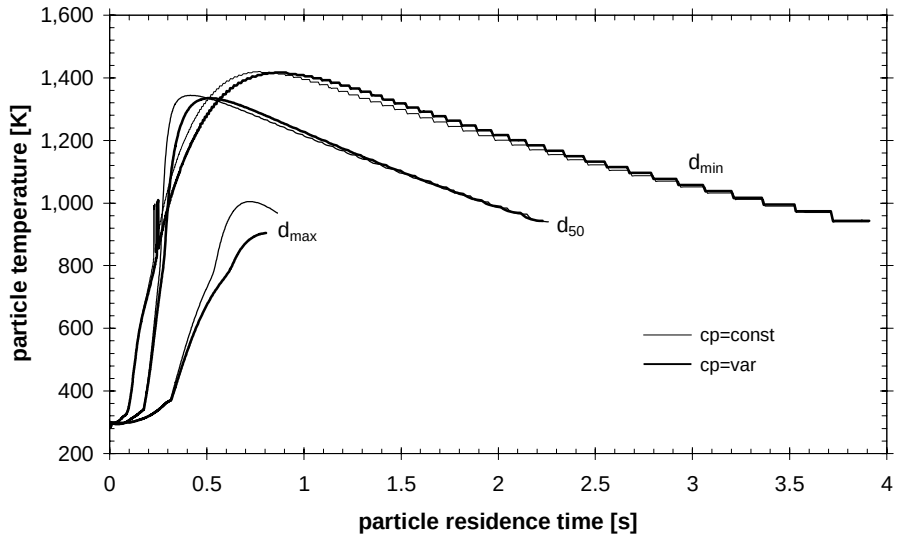

Fig. 5 Calculated particle temperature for three different particle sizes.
Explanations: d_{min}… minimal particle size, value: d_{min}=28.5 [μm]; d_{max}…maximal particle size, value: d_{max} =1,200 [μm]; d_{50}… mean particle size, value: d_{50}=400 [μm]; simulations performed with devolatilization temperature T_{devol}=700 [K] and Magnussen constant A_{mag}=1.

The variable specific heat capacity of the fuel particles c_p influences the flame temperature (Fig. 1) as well as the composition of the gas mixture (Figs. 2-4) only slightly. Fig. 5 shows the effect of a variation of the specific heat capacity of the fuel particles c_p (thick lines) on the particle temperature for three different particle sizes. The thin lines represent the calculation for a constant specific heat capacity of the solid fuel particles c_{sd}. With increasing particle size the influence of a variable specific heat capacity c_p on particle temperature becomes more visible, resulting in lower maximal particle temperatures. At lower particle temperatures less volatiles are released, thus resulting in less combustible gases available in the particle surroundings. According to these results it can be stated, that the appropriate values for the specific heat capacity of the fuel particles are to a lesser extent important for the prediction of the gas phase and to a greater extent important for the evaluation of the particle temperature. A correct prediction of the particle temperature is of great importance, concerning the intention to couple the DPM with an ash deposition model, which is currently under development.

ENGINEERING APPLICATION – BIOMASS FURNACE

The numerically investigated underfeed stoker furnace (nominal capacity related to fuel power input (NCV): 7,000 [kW_{th}]), shown in Fig. 6, operates with wood dust as fuel. The fuel is fed on two separated retorts by two screw conveyors from below. The furnace is subdivided into a short primary combustion zone (oxygen lean atmosphere, air ratio $\lambda < 1$) and a secondary combustion zone (oxygen rich atmosphere, air ratio $\lambda > 1$). For the purpose of temperature control and efficient mixing of unburned flue gas, re-circulated flue gas is supplied below and above the grates.

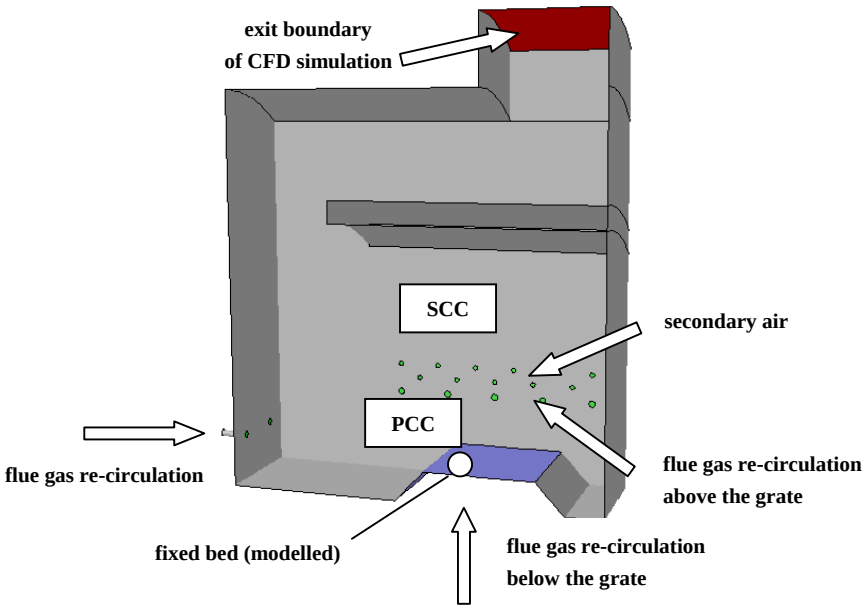

Fig. 6 Sketch of the biomass furnace investigated.
Explanations: PCC…primary combustion chamber; SCC…secondary combustion chamber.

During operation the furnace showed a strong tendency of slag formation, in particular at the upper wall of the primary combustion chamber and on the furnace side walls below it. Due to the slagging and the reaction of the slag with the insulation bricks the capacity of the combustion unit had to be reduced in order to avoid these effects. It is believed, according to the observations made, that the main reason for the above mentioned problem was the fuel itself, because of the small size of the wood dust particles fired (particle size distribution in the range from 40 to 2,000 [μm]). The particles are apparently too small for fixed bed combustion, so that a considerable fraction get entrained from the fuel bed, thus burning not in the bed but "on-the-fly".

In order to investigate this problem two simulations were performed. Both simulations were carried out for nominal boiler load under the assumption of optimum operating conditions (design case) because no measured operating data were available (see Table 5). One simulation (case A) was carried out, assuming that the whole amount of the fuel supplied burns out on the grates. Applying the empirical fixed bed model in a pre-processor mode, the boundary conditions (mass and energy fluxes of the flue gas released from the fuel bed) at the surface of the fixed bed (inlet boundary of the computational domain) were determined for this case. The second simulation (case B) was performed under the assumption that 50 % of the fuel supplied burn out on the grates and the rest gets entrained and burns out "on-the-fly". For this purpose again, the empirical fixed bed model was applied in order to determine the boundary conditions (mass and energy fluxes of the flue gas released from the fixed bed) at the surface of the fixed bed, assumed to contain 50 % of the total amount of the fuel. The remaining 50 % of the total amount of the fuel were injected from the fixed bed (inlet boundary of the computational domain) into the furnace and the combustion process of the injected fuel particles was calculated with the extended DPM model.

Table 5 Operating parameters of the biomass furnace investigated.

parameter	**value**	**unit**
fuel (spruce)	wood dust	-
water content	8	wt% w.b.
nominal capacity	7,000	kW_{th}
recirculation ratio	0.39	-
lambda prim	0.60	-
lambda fuel bed	0.73	-
lambda eff prim	0.98	-
total air ratio	1.6	-
adiabatic flame temperature	1,002	°C

Explanations: nominal capacity…related to fuel power input (NCV); recirculation ratio…mass of flue gas re-circulated / mass of total flue gas in the furnace; lambda prim…primary air ratio based on the total amount of primary air; lamda fuel bed…(effective) air ratio passing through the fuel bed based on the total amount of primary air and re-circulated flue gas supplied below the grate; lambda eff prim…(effective) primary air ratio based on the total amount of primary air and the total amount of re-circulated flue gas; total air ratio…air ratio based on the total amount of injected air (primary and secondary air).

Results

Fig. 7 shows for cases A and B the flue gas temperature distribution in the symmetry plane of the furnace, normalised with the respective gas temperature at furnace exit. It should be noted, that in case B, where the entrained particles were considered, the exit flue gas temperature was lower then in case A, since a part of the fuel particles left the furnace without being burned out completely. Although both simulations show similar results, higher temperatures under the upper wall of the primary combustion chamber (compared to the flue gas temperature at furnace exit) could be detected for case B, which is in accordance with observations. Moreover, the particles partially burn out, when hitting the furnace walls, but without reaching the ash melting temperature (1,300 - 1,400 [°C]).

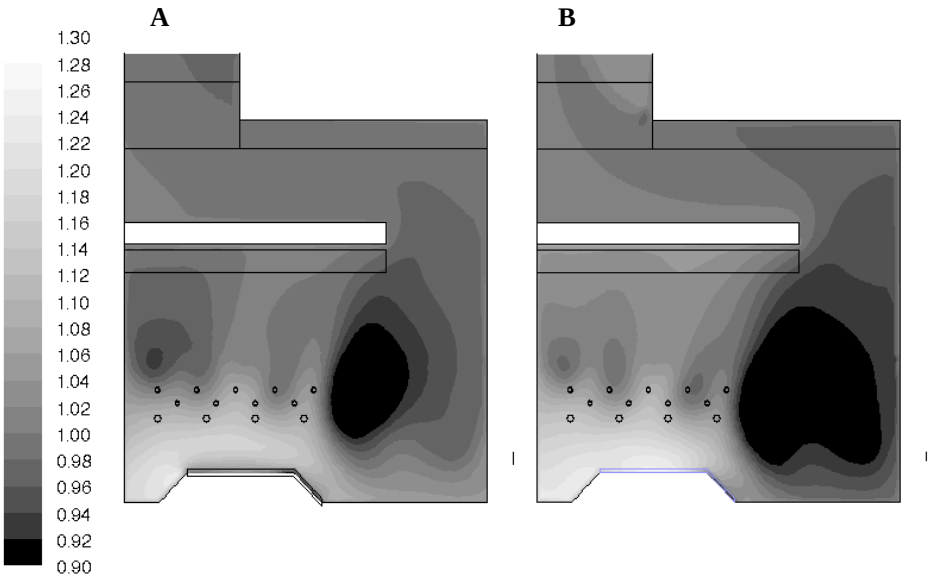

Fig. 7 Normalised flue gas temperature distribution in the symmetry plane of the furnace.

Explanations: temperatures normalised with the respective flue gas temperature at the furnace exit; A- results of the simulation case A; B- results of the simulation case B.

The influence of the entrained fly ash particles was weaker than expected and observed in practice, which is most probably due to the reasons discussed below. When the particles are injected into the furnace from the fuel bed surface they get immediately into the hot temperature zone above the fixed bed. Due to the high temperatures, to which the particles are exposed there, the devolatilisation process occurs rapidly and completes before the particles leave the hot region above the fuel bed. However, the process of char combustion directly under the upper wall of the primary combustion chamber could be predicted. In the simulation performed, the effect of “channeling“ in the fixed bed cannot be modelled by the empirical fixed bed model used [14]. As a consequence, the predicted flue gas temperatures above the fuel

bed are too high. Furthermore, “channeling” contributes to a great extent to the entrainment of the fuel particles. Particles are carried away in strains of a cold gas mixture of primary air and re-circulated flue gas. Thus, in reality the devolatilisation and burnout of the entrained particles takes place not directly above the bed, but in the indicated problem region, resulting in an increase of the temperature of the surrounding flue gas. Furthermore, the size of a certain fraction of the entrained particles cannot be specified as thermally thin. Larger particles (Biot number $Bi < 0.2$ according to [2]) have a delayed thermal response compared to smaller ones and, therefore, behave differently during the combustion process. Without a model, which accounts for the thermally thick nature, the influence of this effect cannot be predicted. Concluding, as already discussed, a model for thermally thick particles is necessary in order to describe the combustion process better.

SUMMARY AND CONCLUSIONS

The development and application of a CFD model for pulverised biomass combustion is presented. The existing Discrete Phase Model (DPM) of the commercial software FLUENT, originally developed for the combustion of pulverised coal, was investigated concerning its capability to predict pulverised wood combustion. Due to the high amount of the volatiles, the devolatilisation process is of the outmost relevance in the case of biomass combustion. Therefore, a more detailed sub-model for the devolatilisation part of the overall conversion process of a single particle was included. Moreover, the original DPM energy equation for a single particle was modified in order to account for the temperature and composition dependent specific heat capacity of a particle during the whole combustion process, i.e. until the state of the inert fly ash.

The extended DPM was validated based on a comparison of experimental data and numerical results of a 2D simulation of a pulverised wood flame. Taking into account the instabilities during experiments, uncertainties have to be assumed for the measurement data when being compared to calculation results. The numerical prediction showed a reasonably good agreement with measurements concerning the flame temperature as well as the O_2 and CO_2 concentrations. The presumed devolatilisation temperature, at which the composition of the volatiles released was determined, does not influence the overall numerical results. An assumption of the composition of the volatiles released, based on an equilibrium composition in the temperature range between 700 to 800 [K] (related to the devolatilisation temperature) is reasonably accurate. The variation of the empirical Magnussen constant showed, that the modelling of the gas phase has a great impact on the overall simulation results. Therefore, more sophisticated gas phase models than the simple EDM, which is not able to account for the complex interaction of turbulence and multi-step reaction kinetics, are currently being implemented and tested. Moreover, the simulations showed, that a more realistic prediction of the particle temperature history could be achieved by the introduction of a variable heat capacity of the fuel particles. A correct prediction of the particle temperature is of great importance in order to couple the DPM with an ash deposition model, which is currently under development.

Moreover, the extended DPM model was applied in combination with an earlier developed empirical fixed bed combustion model for a 3D simulation of a wood dust-fired underfeed stoker furnace in order to investigate the reason for ash slagging

problems, observed during the operation of this plant. By the simulations performed, it turned out that the entrained hot particles, hitting the furnace walls, are most probably the reason for the slagging problems observed, but also indicated that a model describing the combustion of thermally thick particles is needed for a more accurate prediction of the flue gas temperature distribution in the plant.

Concluding, the developed model was successfully tested and applied for the numerical prediction of pulverised wood combustion and showed to be a valuable tool for pulverised biomass combustion furnaces, but further extensions of the model are necessary and ongoing in order to appropriately describe the particle combustion process. Such a model is of great relevance also for co-firing applications as well as for the modelling and prediction of ash deposit formation.

ACKNOWLEDGMENT

The financial support for the research work reported was provided by the European Commission (NNE5-2001-000639, “OPTICOMB”).

REFERENCES

1 Brink A. (1998) Eddy break-up based models for industrial diffusion flames with complex gas phase chemistry. Ph.D. thesis, Abo Akademi University, Finland, ISBN 952-12-0302-1.

2 Bryden K. M., Ragland K. W., Rutland C. J. (2002) Modeling thermally thick pyrolysis of wood. In: Biomass and Bioenergy, Vol. 22, pp. 41-53.

3 FLUENT 6.1 (2003) User’s Guide, Volumes 1-4, Fluent Inc.

4 Grønli M. (1996) A theoretical and experimental study of the thermal degradation of biomass. Ph.D thesis, The Norwegian University of Science and Technology, Norway, Report NTNU 1996:115.

5 Gurgel Veras C. A., Saastamoinen J., Carvalho jr. J. A., Aho M. (1999) Overlapping of the devolatilization and char combustion stages in the burning of coal particles. In: Combustion and Flame, Vol. 116, pp. 567-579.

6 Larfeldt J., Leckner B., Melaaen M. C. (2000) Modelling and measurements of the pyrolysis of large wood particles. In: Fuel, Vol. 79, pp. 1637-1643.

7 Magnussen B. F., Hjertager B. H. (1976) On mathematical modeling of turbulent combustion with special emphasis on soot formation and combustion. In: Proceedings of the 16th Symp. (Int.) on Combustion, pp. 719-729, The Combustion Institute (Ed.), Pittsburgh, USA.

8 Nunn T. R., Howard J. B., Longwell J. P., Peters W. A. (1985) Product compositions and kinetics in the rapid pyrolysis of sweet gum hardwood. In: Industrial & Engineering Chemistry Process Design and Development, Vol. 24, pp. 836-844.

9 Paulrud S., Nilsson C. (2004) The effects of particle characteristics on emissions from burning wood fuel powder. In: Fuel, Vol. 83, pp. 813-821.

10 Scharler R., Obernberger I. (2000) Numerical optimisation of biomass grate furnaces. In: Proceedings of the 5th European Conference on Industrial Furnaces and Boilers, Porto, Portugal, INFUB (Ed.), Rio Tinto, Portugal, ISBN-972-8034-04-0.

11 Scharler R. (2001) Entwicklung und Optimierung von Biomasse-Rostfeuerungen durch CFD-Analyse. Ph.D. thesis, Graz University of Technology, Austria.
12 Scharler R., Obernberger I. (2002) Deriving guidelines for the design of biomass grate furnaces with CFD analysis – a new multifuel-low-NO_x furnace as example. In Proceedings of the 6th European Conference on Industrial Furnaces and Boilers, Estoril-Lisbon, Portugal.
13 Scharler R., Fleckl T., Obernberger I. (2003) Modification of a Magnussen Constant of the Eddy Dissipation Model for biomass grate furnaces by means of hot gas in-situ FT-IR absorption spectroscopy. In: Progress in Computational Fluid Dynamics, Vol. 3, Nos. 2-4, pp. 102-111.
14 Scharler R., Widmann E., Obernberger I. (2004) CFD Modelling of NO_x formation in biomass grate furnaces with detailed chemistry. To be published in Proceedings of the 6th International Conference in Science in Thermal and Chemical Biomass Conversion, Vancouver, Canada.
15 Tao L., Berge N., Elfasakhany A., Bai X. S. (2002) Experimental and numerical studies of a pulverised wood flame. In: Proceedings of the 6th European Conference on Industrial Furnaces and Boilers, Estoril-Lisbon, Portugal.
16 Williams A., Pourkashanian M., Jones J. M (2001) Combustion of pulverised coal and biomass. In: Progress in Energy and Combustion Science, Vol. 27, pp. 587-610.